J. Chem. Sci. (2024)136:27
https://doi.org/10.1007/s12039-024-02260-y

REGULAR ARTICLE

Crystallization of zinc azole complex incorporated Strandberg-type cluster-based solids: Synthesis, structure and photoluminescence studies

RAJI CHORENJETH RADHAKRISHNAN[a], JISHA JOSEPH[a], MANISHA JADON[b], MEMSY CHIRIAMKANDATH KURIAKOSE[c] and JENCY THOMAS[a,*]

[a]Centre for Sustainability Science, Research & PG Department of Chemistry, St. Thomas College (Autonomous), Affiliated to University of Calicut, Thrissur, Kerala 680001, India
[b]Department of Chemistry, Indian Institute of Technology Delhi, Hauz Khas, New Delhi 110016, India
[c]Research & PG Department of Chemistry, Mercy College, Affiliated to University of Calicut, Palakkad, Kerala 678006, India
E-mail: jencythomas@stthomas.ac.in

MS received 15 November 2023; revised 12 January 2024; accepted 18 January 2024

Abstract. Two new zinc azole complexes incorporated Strandberg-type cluster-based solids, namely $(Hpz)_6\{Zn(pz)_4(H_2O)_2\}[\{Zn(pz)_2P_2Mo_5O_{23}\}_2]\cdot 8H_2O$ (**1**) and $(Himi)_4\{Zn(imi)_3P_2Mo_5O_{23}\}\cdot 7H_2O$ (**2**) were crystallized using isomeric azole ligands, i.e., pyrazole (*pz*) and imidazole (*imi*), respectively. While solid **1** crystallized in triclinic system with space group *P*-1 with cell parameters a = 9.5647(15), b = 12.558(2), c = 20.340(3) Å, α = 75.907(7), β = 84.727(6), γ = 87.525(7)°, Z = 1; **2** crystallized in orthorhombic system with space group $P2_12_12_1$ having cell parameters a = 12.048(3), b = 19.561(5), c = 20.732(5) Å, Z = 4. Both pyrazole and imidazole can form a complex with zinc centres to form an extended solid in **1** and a derivatized Strandberg-type cluster in **2**. Interestingly, **1** is a new supramolecular isomer of previously reported solid viz., $(pz)[\{Zn(pz)_3\}_3\{P_2Mo_5O_{23}\}]\cdot 2H_2O$ and **2** is the only example wherein a zinc imidazole complex has derivatized a Strandberg-type cluster. Detailed structure analysis of **1** and **2** was carried out, and the role of tectons in dictating the self-assembly of these solids was evaluated. In addition, a solid-state photoluminescence study was carried out for **1** and **2** at room temperature.

Keywords. Phosphomolybdate cluster; zinc azole complex; supramolecular interactions; photoluminescence studies.

1. Introduction

During the last decade, our group has been examining the reaction conditions wherein *in-situ* generated phosphomolybdate cluster anion viz., Strandberg-type $\{P_2Mo_5O_{23}\}^{6-}$ crystallizes along with organic cations and/or metal complexes.[1–3] It has been observed that cluster anion $\{P_2Mo_5O_{23}\}^{6-}$ can either occur as discrete anion and crystallize with organic cations or metal complexes or condense through extended –metal–(O_t-cluster-O_t)–metal– bonds into multi-dimensional coordination frameworks.[4–6] Occasionally, self-assembly also results in structures wherein the $\{P_2Mo_5O_{23}\}^{6-}$ cluster gets derivatized with metal complexes.[7,8] In rare cases, the metal centres form an extended network (such as coordination polymers) incorporating the cluster anion.[9,10] In all these cases, the nature of metal centres and organic ligands is crucial. While the organic ligands can act as buffers, reducing agents, and templating agents,[11,12] the metal centres can exhibit multiple oxidation states, various coordination geometries, and even manifest catalytic, magnetic, or optical properties to the solids.[13–16]

Our initial investigations involved the self-assembly of $\{P_2Mo_5O_{23}\}^{6-}$ cluster-based solids and copper pyrazole complexes under ambient conditions.[17] Six different solids were obtained by varying copper:pyrazole ratio. It was evident that non-bonding

*For correspondence
Supplementary Information: The online version contains supplementary material available at https://doi.org/10.1007/s12039-024-02260-y and www.ias.ac.in/chemsci.

Published online: 13 April 2024

interactions between the complexes and $\{P_2Mo_5O_{23}\}^{6-}$ cluster anions dictated the formation of a particular solid. The results were further explored by varying the pH and temperature of the reaction medium.[18] Subsequently, the complexing ability of other transition metal ions with pyrazole was exploited to crystallize $\{P_2Mo_5O_{23}\}^{6-}$ cluster-based solids (pH and temperature kept constant).[19] The study revealed that zinc behaves slightly differently from the rest of the transition metal ions. Firstly, the predominant coordination number for zinc was four or five. Secondly, being more basic than other first-row transition metal ions, it formed other competitive phases, such as zinc phosphates. This is also reflected in terms of a limited number of Zn(II) complex incorporated $\{P_2Mo_5O_{23}\}^{6-}$ cluster-based solids as compared to other first-row transition metal complexes (refer Scheme 1; also refer Table S1, Supplementary Information). Therefore, the objective of the present work was to investigate the crystallization of zinc complex incorporated $\{P_2Mo_5O_{23}\}^{6-}$ cluster-based solids and systematically vary the reaction parameters to examine the growth of new solids. Under our reaction conditions, two solids containing Strandberg-type $\{P_2Mo_5O_{23}\}^{6-}$ cluster anion and zinc azole (pyrazole, *pz* and imidazole, *imi*) complex were obtained. Interestingly, solvent evaporation technique resulted in $(Hpz)_6\{Zn(pz)_4(H_2O)_2\}[\{Zn(pz)_2P_2Mo_5O_{23}\}_2]\cdot 8H_2O$ (**1**) a new supramolecular isomer[20] of previously reported solid $(pz)[\{Zn(pz)_3\}_3\{P_2Mo_5O_{23}\}]\cdot 2H_2O$.[19] Therefore, the same reaction was carried out using its position isomer, namely imidazole and $(Himi)_4\{Zn(imi)_3P_2Mo_5O_{23}\}\cdot 7H_2O$ (**2**) was obtained. Interestingly, **2** is the only example of a zinc imidazole complex derivatized Strandberg-type cluster. A detailed structure analysis of **1** and **2** could provide insights into how one could crystallize new solids by changing the nature of reacting molecular precursors (tectons). Further, the photoluminescence of **1** and **2** was also measured in the solid state. The results are significant as only a few examples of zinc complex incorporated $\{P_2Mo_5O_{23}\}^{6-}$ cluster-based solids are known. Also, the results indicated that the emission intensity and wavelength in the Strandberg-type cluster could be tuned by both zinc complex and organic ligands.

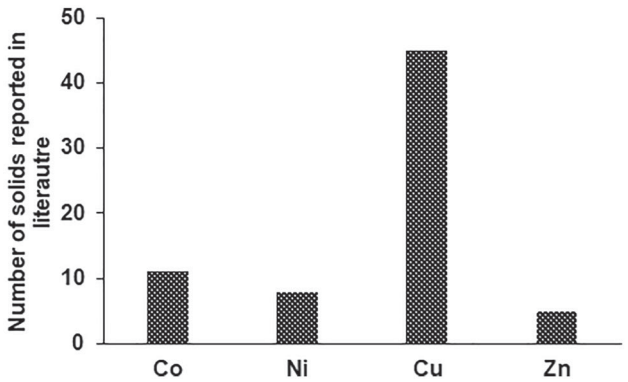

Scheme 1. A preview of Strandberg-type cluster-based solids incorporating Co, Ni, Cu, and Zn complexes.

2. Experimental

2.1 *Synthesis*

$ZnCl_2$ (1.65 mmol, Merck) and pyrazole (4.95 mmol, Aldrich) were dissolved in 20 mL of distilled water and added to 20 mL of aqueous solution of $Na_2MoO_4\cdot 2H_2O$ (1.65 mmol, Merck) kept under stirring. Immediately, a turbidity was observed. It was dissolved using 1M H_3PO_4 (Merck, 85%). Solvent evaporation of the resultant solution (pH $\sim$ 1) resulted in needle-shaped crystals of **1** (yield: 70–75% based on Mo). The same procedure was repeated for synthesizing **2** using imidazole (4.95 mmol, Aldrich) instead of pyrazole (yield: 70–75% based on molybdenum).

2.2 *Characterization*

CHN analysis was carried out using ELEMENTAR Vario EL III CHNS Analyzer. Anal. Found: C, 20.59; H, 2.56; N, 12.38%: Calcd: C, 20.54; H, 2.60; N, 12.43% for **1** and C, 16.01; H, 2.86; N, 12.34%: Calcd: C, 15.93; H, 2.91; N, 12.39% for **2**. Fourier transform infrared (Shimadzu FTIR spectrophotometer) spectra of solids displayed characteristic bands of molybdenum oxygen stretching (650–690, 750–830 and 900–930 cm^{-1}), P–O stretching (1000–1100 cm^{-1}), N-H bending (1400–1420 cm^{-1}), C–H bending (1620–1640 cm^{-1}) and O–H stretching (3100–3400 cm^{-1}) vibrations (refer Figure S1 (SI) for details of bands for **1** and **2**).[21] The solids were also characterized using powder X-ray diffraction (Malvern Panalytical Aeris diffractometer) and thermogravimetric analysis (Perkin-Elmer TGA7). UV-visible spectral data of **1**, **2**, and ligands in solid state was collected using a UV-visible spectrophotometer (UV-2600 spectrometer, Shimadzu, Japan). Photoluminescence studies (PL) were carried out using a Shimadzu Spectro flouro photometer (RF-5301PC). BRUKER AXS SMART-APEX diffractometer was used for X-ray crystallographic studies. Frames were collected using SAINT.[22] The absorption corrections were

carried out with SADABS.[23] SHELXTL program was used for structure solution and refinement.[24] Hydrogen bonding interactions were calculated using DIAMOND.[25] Details of characterization techniques and X-ray crystallographic studies are available in Scheme S1 (SI) (also refer to Table 1).

3. Results and discussion

3.1 *Crystal structure of* (**1**) *and* (**2**)

The asymmetric units of $(Hpz)_6\{Zn(pz)_4(H_2O)_2\}[\{Zn(pz)_2P_2Mo_5O_{23}\}_2]\cdot 8H_2O$ (**1**) consists of two sets of zinc complexes (represented by Zn1 and Zn2), $\{P_2Mo_5O_{23}\}^{6-}$ cluster anion (denoted as $\{P_2Mo_5\}$ for simplicity) and protonated pyrazole moieties. The structure of $\{P_2Mo_5O_{23}\}^{6-}$ cluster anion is the same as that reported earlier by Strandberg and others.[26–28] The distorted tetrahedral zinc complex, $\{Zn1(pz)_2O_2\}$, covalently links adjacent $\{P_2Mo_5\}$ clusters into linear chains propagating along *a* axis (Figure 1 and Table S2, SI). The $(Hpz)^+$ cation moieties as well as lattice water molecule, O4W are anchored to the chain through N-H···O interactions (1.782(6)–2.177(4) Å, Figure 2(a) and Table S3, SI). These 1-D chains further aggregate through H-bonding interactions with octahedral $\{Zn2(pz)_4(H_2O)_2\}^{2+}$ complex to form a double chain (Figure 2b). While O1W constitutes the axial bonds of octahedral $\{Zn2(pz)_4(H_2O)_2\}^{2+}$ complex; lattice water molecule, O5W is associated with the complex *via* H-bonding interactions. The neighboring double chains are connected *via* O···O interactions (3.040(11)–3.195(10) Å) mediated through lattice water molecules (trimeric water cluster of O2W, O3W, and O4W) to form supramolecular 2-D sheets (Figure S2, SI). CH…π interaction (3.231(8) Å) between neighboring sheets mediated by {N3N4} and {N9N10} pyrazole moieties facilitates the 3-D crystal packing in **1** (Figure S3, SI).

Crystal structure analysis of $(Himi)_4\{Zn(imi)_3P_2Mo_5O_{23}\}\cdot 7H_2O$ (**2**) indicated the presence of zinc imidazole complex derivatized $\{P_2Mo_5\}$ cluster, four protonated imidazole moieties and seven water molecules per asymmetric unit of **2** (Figure 1(b)). The zinc imidazole complex derivatizes the cluster through Zn–O coordination to form $\{Zn(imi)_3P_2Mo_5O_{23}\}$ unit, which further aggregates through non-bonding interactions with four $(Himi)^+$ cations. The protonated imidazole moieties {N13N14} link neighboring $\{Zn(imi)_3P_2Mo_5O_{23}\}$ cluster anions through H-bonding interactions (1.801(4)–1.880(4) Å) to form 1-D chains as shown in Figure 3(a). The adjacent chains are further connected through {N11N12} moieties and lattice water molecules (forming a pentameric water cluster) to form 3-D network, as shown in Figure 3(b). In the water cluster, the O···O distances were observed at 2.694(13)-3.057(12) Å (refer to Table S5 and S6 (SI) for H-bonding and O···O interactions, respectively). CH···π interactions along *a* axis between zinc imidazole complexes of neighboring 1-D chains, along with CH···π interactions between {N11N12} moiety and {N5N6} of the zinc complex, further stabilize the formation of 3-D network (refer Figure 4

Table 1. Crystallographic details for **1** and **2**.

	1	**2**
Formula	$C_{54}H_{64}Mo_{10}N_{28}O_{56}P_4Zn_3$	$C_{21}H_{32}Mo_5N_{14}O_{30}P_2Zn$
Formula weight	3136.66	1567.64
T (K)	293	298
Space Group	*P*-1	$P2_12_12_1$
a, Å	9.5647(15)	12.048(3)
b, Å	12.558(2)	19.561(5)
c, Å	20.340(3)	20.732(5)
α, °	75.907(7)	90.00
β, °	84.727(6)	90.00
γ, °	87.525(7)	90.00
V, Å^3	2359.0(6)	4886(2)
Z	1	4
d_{calc}, g·cm^{-3}	2.208	2.131
$\mu_{MoK\alpha}$, cm^{-1}	2.209	1.899
λ (Å)	0.71073	0.71073
$R_1(I>2\sigma I)$, WR_2(all)	0.0590, 0.1534	0.0583, 0.1070
GOF	1.063	1.231
Largest difference map hole and peak (eÅ^{-3})	−3.150, 1.630	−0.719, 1.013
CCDC No.	2299536	2299537

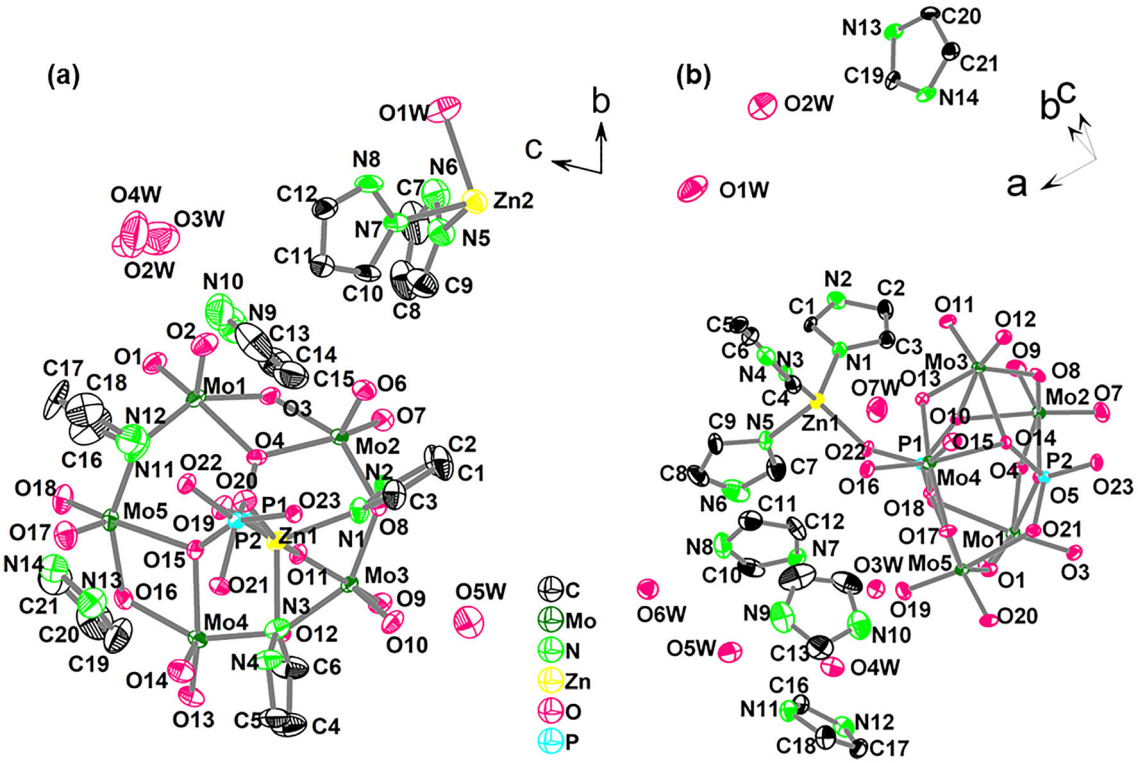

Figure 1. ORTEP diagram of (a) **1** and (b) **2**.

and Table S7, SI). In addition, π···π interaction between three of the protonated (H*imi*)$^+$ moieties viz., {N7N8}, {N9N10} and {N13N14} reinforce the crystal packing in **2**, as shown in Figures S4 and S5 (SI).

3.2 *Analysis of solids* **1** *and* **2**

Thermogravimetric analysis of **1** and **2** (Figure S6, SI) showed weight loss in three steps. In **1**, the first weight loss up to 120 °C, corresponding to 4.7%, could be ascribed to the loss of lattice water molecules (theoretical value: 4.56%). It was followed by a weight loss of 31.1% (theoretical value: 30.21%) corresponding to thermal degradation of pyrazole moieties. The third weight loss (above 780 °C) could be assigned to the decomposition of cluster anion. On the contrary, **2** showed an initial weight loss of 7.82% (theoretical value: 7.97%) at 100 °C, corresponding to the loss of seven lattice water molecules. It was followed by the thermal degradation of imidazole moiety, corresponding to a weight loss of 31.42% (theoretical value: 30.13%). The third weight loss could be attributed to the decomposition of cluster anions.

In both **1** and **2**, the phase purity of the solids was established by comparing the experimental powder X-ray diffraction (PXRD) pattern with the simulated powder pattern of the single crystal structure, as shown in Figures S7-S8 (SI).

3.3 *Photoluminescence studies*

The UV–vis spectra of solids **1** and **2** showed intense bands at 210–220 and 245–255 nm. It could be attributed to transitions corresponding to ligand moiety and pπ–dπ (O→Mo) charge transfer transition in Strandberg-type cluster anion, respectively (Figure S9, SI). The photoluminescence property of the free ligands as well as the solids **1** and **2**, was investigated at room temperature (Figure 5). Both pyrazole and imidazole exhibited a comparatively weak emission at 370 nm upon photoexcitation at 220 nm, which could be assigned to ligand-centered π–π* transition.[29,30] In **1** and **2**, it was observed that the emission intensity of the hybrid solids was enhanced as compared to the free ligand. This could be attributed to the rigidity in the solids after the ligand is coordinated with zinc ions, which reduces energy loss through radiationless decay.[31–33] Since Zn^{2+} ions are difficult to oxidize or reduce (on account of their d^{10} configuration), metal-to-ligand charge transfer (MLCT) and ligand-to-metal charge transfer (LMCT) could be ignored.[32] Therefore, the emission spectra could be ascribed to intra-

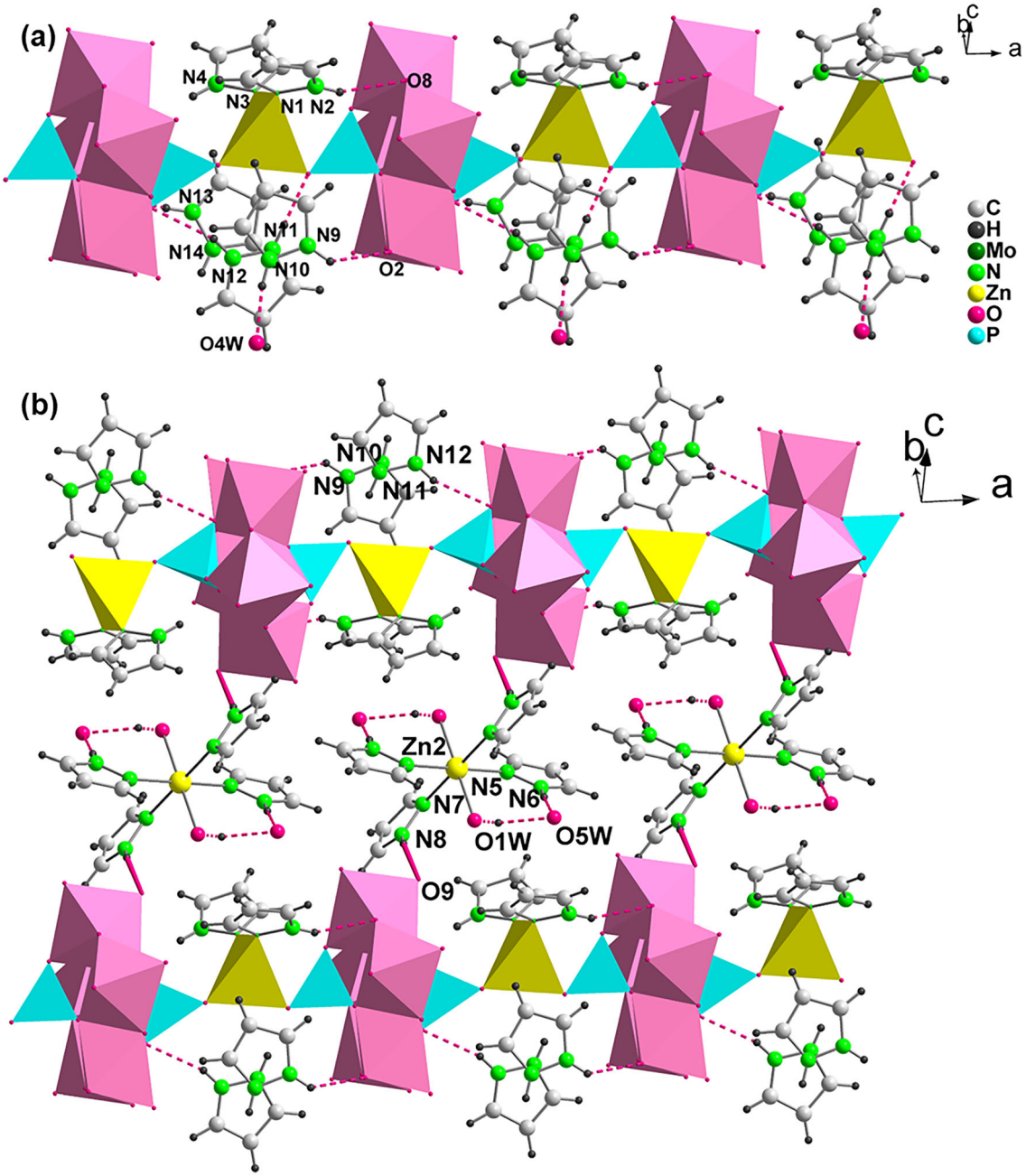

Figure 2. (a) 1-D chains formed between distorted tetrahedral zinc complex, $\{Zn1(pz)_2O_2\}$ and $\{P_2Mo_5\}$ cluster anions. The $(Hpz)^+$ cation moieties *viz.* {N9N10}, {N11N12} and {N13N14} as well as lattice water molecule, O4W are attached to the chain through N–H···O interactions (shown in dashed red lines). (b) The 1-D chains are further connected through H-bonding interactions (shown in solid red lines) mediated by octahedral $\{Zn2(pz)_4(H_2O)_2\}^{2+}$ complex to form a double chain. {N13N14} moiety has been omitted for clarity.

ligand and ligand-to-ligand charge transition (LLCT) as suggested by Liu *et al.* [32] Interestingly, while solid **1** exhibited a comparatively strong emission at 372 nm upon excitation at 245 nm, a blue shift of 14 nm in the emission wavelength of solid **2** as compared to the free ligand was observed. It could be attributed to the coordination effect of imidazole, "which increases the ligand conformational rigidity and asymmetry of the ligands, thereby reducing the non-radiative decay of the intra ligand excited state" as suggested by Zhang *et al.*[34]

3.4 *Chemistry of formation*

In the present work, an acidic medium of molybdate and phosphate precursors, zinc ions, and azole ligands was allowed to crystallize *via* solvent

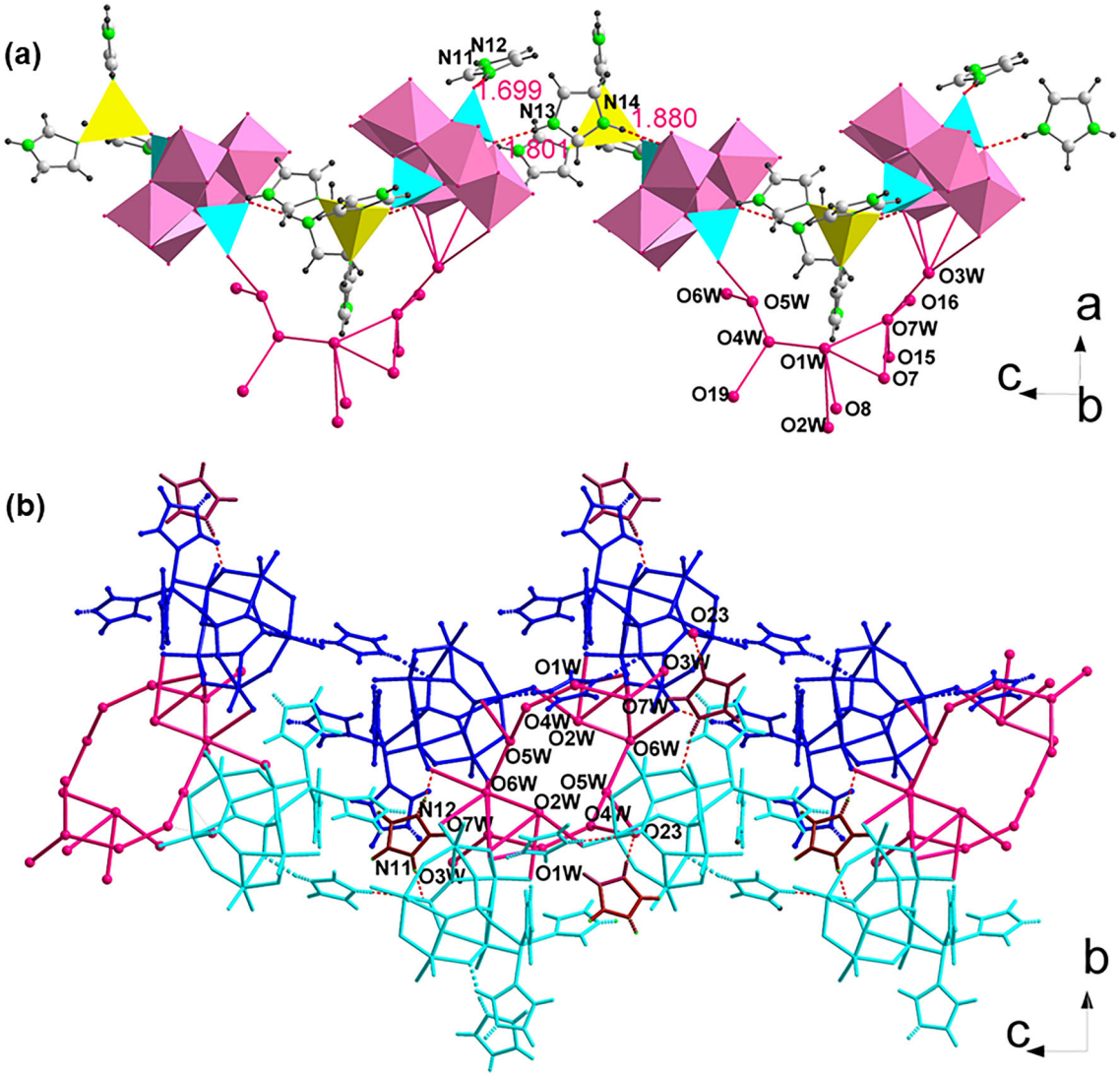

Figure 3. (a) 1-D chains formed *via* H-bonding interactions mediated by protonated imidazole moieties {N13N14}. Hydrogen-bonding interactions are shown in dashed red lines. O1-6W represents the associated lattice water molecules. The interactions between them (O···O) have been depicted in a solid pink color. (b) NH···O interactions mediated by {N11N12} moiety (shown in brown color) along with lattice water molecules link neighboring chains. Two such neighboring chains are shown here in cyan and blue color. Dashed red lines represent the inter-chain NH···O interactions.

evaporation. The low pH favored the protonation of the organic ligands (pyrazole: pK_a = 2.1; imidazole: pK_a = 6.8).[35] Therefore, only a few ligand moieties could complex with zinc ions to form the solids **1** and **2** (equation (i)):

$$\{P_2Mo_5O_{23}\}^{6-} + (HL)^{+} + \{Zn(L)_n(H_2O)_m\}^{2+} \rightarrow \mathbf{1} \quad \text{and} \quad \mathbf{2} \qquad \text{(i)}$$

However, the nature of the zinc complex incorporated in solids **1** and **2** was different. The formation of zinc ligand complex can be visualized as a step-by-step process, and at any instance, the reaction medium would have more than one kind of zinc ligand complex:

$$\left[Zn(H_2O)_6\right]^{2+} \rightleftharpoons \left[ZnL(H_2O)_5\right]^{2+} \rightleftharpoons \left[ZnL_2(H_2O)_4\right]^{2+} \rightleftharpoons \left[ZnL_3(H_2O)_3\right]^{2+} \rightleftharpoons \left[ZnL_4(H_2O)_2\right]^{2+} \qquad \text{(ii)}$$

Thus, during the formation of solid **1**, the tectons (reacting molecular precursors)[36] viz., $[Zn1(pz)_2(H_2O)_4]^{2+}$ and $[Zn2(pz)_4(H_2O)_2]^{2+}$ along with $(Hpz)^{+}$ units aggregate with $\{P_2Mo_5O_{23}\}^{6-}$ ions to form extended chains in **1**. Zn1 centers exhibit tetrahedral geometry in the solid state and connect the adjacent $\{P_2Mo_5\}$ cluster anions to form chains. On the other hand, $[Zn2(pz)_4(H_2O)_2]^{2+}$ units appear as countercations in **1**. However, in the case of imidazole, when $[Zn(imi)_3(H_2O)_3]^{2+}$ tectons aggregate along with

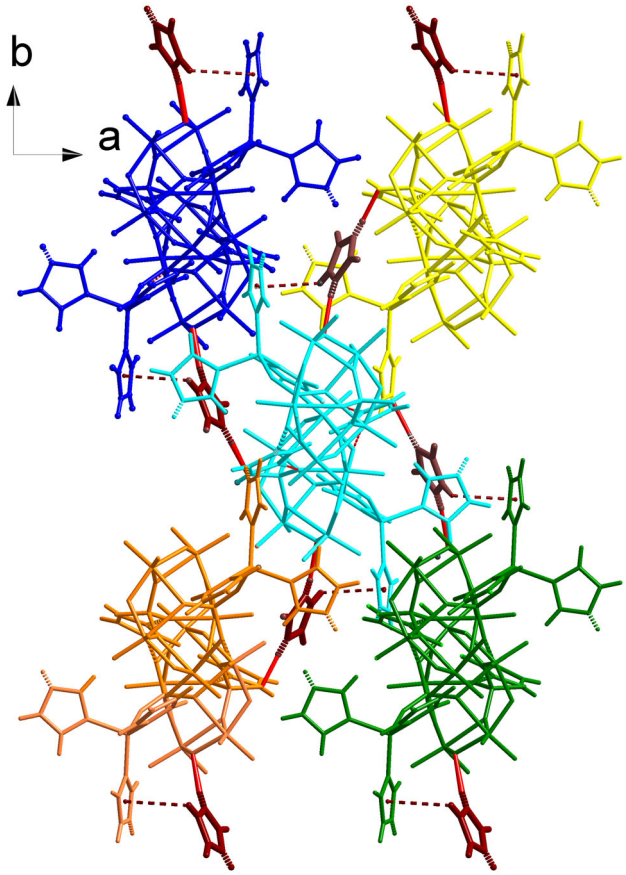

Figure 4. View along *c* axis showing a connection between one 1-D chain (depicted in cyan) with four others through {N11N12} moiety (shown in brown color) and lattice water molecules. The lattice water molecules have been removed for clarity. Inter-chain NH···O interactions are shown in solid red lines. CH···π interactions between {N11N12} moiety and {N5N6} of the zinc complex are shown in dashed brown lines.

$(H\textit{imi})^{+}$ and $\{P_2Mo_5O_{23}\}^{6-}$ units, zinc imidazole complex derivatizes the $\{P_2Mo_5\}$ cluster anion by adopting a tetrahedral geometry. Therefore, **2** exists as a discrete cluster rather than an extended coordinated solid. During aggregation, one has no control over the type of tecton that would participate in the self-assembly. Crystal packing effects are driven by favorable non-covalent interactions, which facilitate the aggregation of appropriate tectons to form solids **1** and **2**. However, the presence of the acidic medium ensures the incorporation of protonated ligand moieties along with metal complexes in the crystal structure. Thus, slight variations in reaction conditions (particularly pH, concentration of reactants, and temperature) could result in the crystallization of new solids. The molar ratio of the reactants plays an important role in determining the nature of aggregating tectons in solution. For example, in an acidified reaction medium containing $ZnCl_2$ and *imi*, a high *imi*: Zn ratio seems to favor the formation of $[Zn(\textit{imi})_x(H_2O)_y]^{2+}$ tectons (where x = 3–6), leading to solids $[Zn(\textit{imi})_6Cl_2]\cdot 4H_2O$ and $(H\textit{imi})_4\{Zn(\textit{imi})_3P_2Mo_5O_{23}\}\cdot 7H_2O$, **2** (Table S8, SI). On the other hand, if a low *imi*: Zn ratio is used during the synthesis (involving solution acidified with HCl); the predominant tectons would plausibly be $[ZnCl_4]^{2-}$ and $[Zn(\textit{imi})_x(H_2O)_y]^{2+}$ (where x = 0–2) resulting in crystallization of solids such as $[H_2\textit{imi}]_2[ZnCl_4]$ and $[NBu_4][PMo_{12}O_{37}(OH)_3Zn_4(\textit{imi})(H\textit{imi})]$.

It is noteworthy that $(Hpz)_6\{Zn(pz)_4(H_2O)_2\}[\{Zn(pz)_2P_2Mo_5O_{23}\}_2]\cdot 8H_2O$ (**1**) is a new supramolecular isomer of $(pz)[\{Zn(pz)_3\}_3\{P_2Mo_5O_{23}\}]\cdot 2H_2O$.[19] The latter was crystallized using a hydrothermal technique at pH ∼ 7. The molar ratio of Mo:Zn:L in the reactants was taken as 3:1:6 rather than 1:1:3 (used in the present study). At pH ∼ 7, pyrazole moieties mainly exist as neutral species. Besides, it has been observed that aggregation of lattice water molecules seems favorable if synthesis is carried out at room temperature. Therefore, the formation of less hydrate

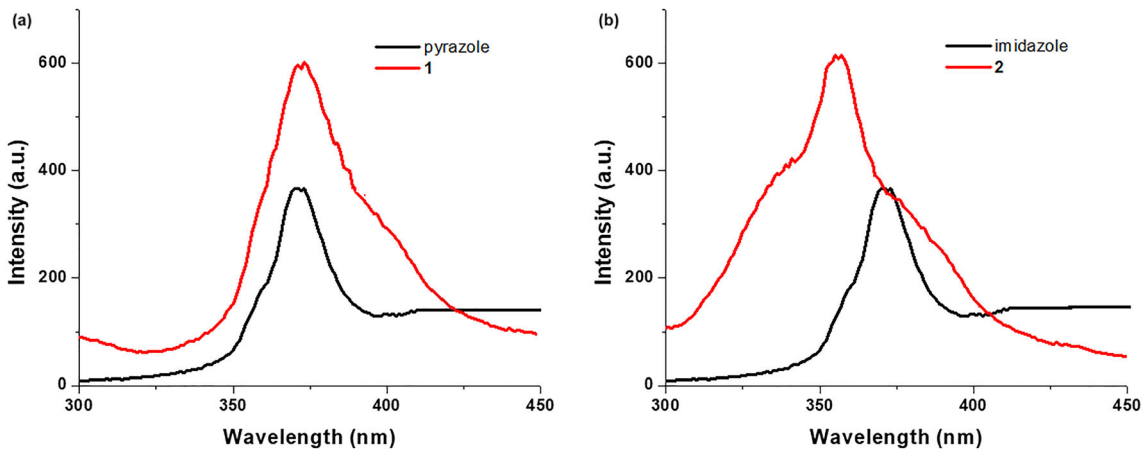

Figure 5. PL spectra of (a) pyrazole and **1** and (b) imidazole and **2**.

supramolecular isomers viz., $(pz)[\{Zn(pz)_3\}_3\{P_2Mo_5O_{23}\}]\cdot 2H_2O$ under hydrothermal conditions seems obvious. The high *pz*: Zn ratio most likely favored the formation of $[Zn(pz)_3(H_2O)_3]^{2+}$ tectons and resulted in the solid $(pz)[\{Zn(pz)_3\}_3\{P_2Mo_5O_{23}\}]\cdot 2H_2O$. On the contrary, the low *pz*: Zn ratio used in the present synthesis results in the incorporation of $[Zn(pz)_2(H_2O)_4]^{2+}$ tectons during the crystallization of **1**. The change in molar ratio of reactants also resulted in variation in zinc complex: $\{P_2Mo_5O_{23}\}^{6-}$ ratio in the synthesized solids. It was found to be 1.5:1 in $(Hpz)_6\{Zn(pz)_4(H_2O)_2\}[\{Zn(pz)_2P_2Mo_5O_{23}\}_2]\cdot 8H_2O$ (**1**) as compared to 3:1 in $(pz)[\{Zn(pz)_3\}_3\{P_2Mo_5O_{23}\}]\cdot 2H_2O$. In $(Himi)_4\{Zn(imi)_3P_2Mo_5O_{23}\}\cdot 7H_2O$ (**2**), zinc complex: $\{P_2Mo_5O_{23}\}^{6-}$ ratio was 1:1.

4. Conclusions

Our results suggest that subtle variations in synthetic protocols can influence the formation of new solids. In the present study, slow evaporation of a solution containing molybdate and phosphate precursors in the presence of zinc ions and azole ligands resulted in two new zinc azole complex-based phosphomolybdates. Structural analysis of the solids revealed that non-bonding interactions direct the self-assembly of molecular units, reinforcing the crystal packing in such solids. The synthesized solids also exhibited intense emissions at room temperature, suggesting they may be good candidates for a potential photoactive material.

Supplementary Information (SI)

Literature preview; details of characterization techniques and x-ray crystallographic study; tables and figures showing non-covalent interactions in **1** and **2**; FTIR spectra; TGA curves; comparison of simulated and experimental PXRD patterns are available at www.ias.ac.in/chemsci. CCDC 2299536 and 2299537 contain the supplementary crystallographic data for **1** and **2**. The data can be obtained freely via http://www.ccdc.cam.ac.uk/data_request/cif, or by e-mailing to data_request@ccdc.cam.ac.uk or by contacting the Cambridge Crystallographic Data Centre (12 Union Road, Cambridge CB2 1EZ, UK. Fax: +44 1223 336033) directly.

Acknowledgments

JT sincerely acknowledges her mentor, Prof. A. Ramanan, former Professor of the Department of Chemistry, Indian Institute of Technology (IIT), Delhi, for his guidance and support over the years. JT thanks UGC for research project 2243-MRP/15-16/KLCA019/UGC-SWRO. JT and JJ thank St. Thomas College (Autonomous), Thrissur, for providing seed money STC/SANTHOME/SEEDMONEY/2020-21/14 and STC/SANTHOME/SEEDMONEY/2020-21/17 respectively. The authors acknowledge DST and UGC for the FIST and CPE programs implemented in St. Thomas College (Autonomous), Thrissur. The authors wish to thank the Department of Chemistry, IIT Delhi, for providing a smart apex CCD single crystal X-ray diffractometer under FIST for collecting data of solids **1** and **2**. The authors acknowledge the Sophisticated Test and Instrumentation Centre (STIC), Cochin University, for making CHN analyses and thermogravimetric analysis available.

References

1. Thomas J 2010 Ph.D. Thesis, Indian Institute of Technology, Delhi, India
2. Joseph J, Winson C, Singh B, Jose J and Thomas J 2020 Role of supramolecular interactions in crystal packing of Strandberg-type cluster-based hybrid solids *J. Chem. Sci.* **132** 137
3. Joseph J 2021 Ph.D. Thesis, University of Calicut, Kerala, India
4. Ganesan S V and Natarajan S 2005 Hydrothermal synthesis and structure of $[(C_4N_2H_{12})_3][P_2Mo_5O_{23}]\cdot H_2O$ and $[(C_3N_2H_{12})_3][P_2Mo_5O_{23}]\cdot 4H_2O$ *J. Chem. Sci.* **117** 219
5. Zhang C X, Chen Y G, Tang Q, Zhang Z C, Liu D D and Meng H X 2012 Self-assembly of high-dimensional architecture from Strandberg-type polyoxometalate clusters and silver ions *Inorg. Chem. Commun.* **17** 155
6. Paul L, Dolai M, Panja A and Ali M 2016 Hydrothermal synthesis of two supramolecular inorganic–organic hybrid phosphomolybdates based on Ni(II) and Co(II) ions: structural diversity and heterogeneous catalytic activities *New J. Chem.* **40** 6931
7. Jin H J, Zhou B B, Yu Y, Zhao Z F and Su Z H 2011 Inorganic–organic hybrids constructed from heteropolymolybdate anions and copper–organic fragments: syntheses, structures and properties *CrystEngComm* **13** 585
8. Ammari Y, Dhahri E, Rzaigui M, Hlil E K and Abid S 2016 Synthesis, Structure and Physical Properties of an Hybrid Compound Based on Strandberg Type Polyoxoanions and Copper Cations *J. Clust. Sci.* **27** 1213
9. Lu Y, Li Y, Wang E, Lü J, Xu L and Clérac R 2005 $[H_2bpy]_2[\{Cu(btepy)_2\}Mo_5P_2O_{23}]\cdot 4H_2O$: A Three-Dimensional Framework Built from Transition-Metal Coordination Polymer Sheets Pillared by Polyoxomolybdophosphate Clusters *Eur. J. Inorg. Chem.* 1239
10. Wu T, Liao M, Wang Y, He S and Xie Y 2021 Controllable syntheses of metal-organic frameworks based on Strandberg-type $[P_2Mo_5O_{23}]$ cluster *J. Solid State Chem.* **303** 122541
11. Joshi A, Gupta R, Singh B, Sharma D and Singh M 2020 Effective inhibitory activity against MCF-7, A549 and HepG2 cancer cells by a phosphomolybdate based hybrid solid *Dalton Trans.* **49** 7069

12. Asnani M, Kumar D, Duraisamy T and Ramanan A 2012 Crystallization of organically templated phosphomolybdate cluster-based solids from aqueous solution *J. Chem. Sci.* **124** 1275
13. Ji Y M, Fang Y, Han P P, Li M X, Chen Q Q and Han Q X 2017 Copper(II) and cadmium(II) complexes derived from Strandberg-type polyoxometalate clusters: Synthesis, crystal structures, spectroscopy and biological activities *Inorg. Chem. Commun.* **86** 22
14. Wu L, Ma H, Han Z and Li C 2009 Synthesis, structure and property of a new inorganic-organic hybrid compound $[Cu(phen)_2][Cu(phen)H_2O]_2[Mo_5P_2O_{23}]\cdot 3.5H_2O$ *Solid State Sci.* **11** 43
15. Hu G, Dong Y, He X, Miao H, Zhou S and Xu Y 2015 Hydrothermal synthesis, structure and properties of two new phosphomolybdates based on Strandberg-type $\{P_2Mo_5O_{23}\}^{6-}$ building units *Inorg. Chem. Commun.* **60** 33
16. Lu Y, Lü J, Wang E, Guo Y, Xu X and Xu L 2005 Two novel diphosphopentamolybdate cluster supported transition metal complexes: $(H_2bpy)_{0.5}\{[Ni(H_2O)_5][Ni(Hbpy)(H_2O)_4][Mo_5P_2O_{23}]\}$ and $(H_2bpy)_{0.5}\{[Co(H_2O)_5][Co(Hbpy)(H_2O)_4][Mo_5P_2O_{23}]\}$ *J. Mol. Struct.* **740** 159
17. Thomas J and Ramanan A 2008 Growth of copper pyrazole complex templated phosphomolybdates: Supramolecular interactions dictate nucleation of crystal *Cryst. Growth. Des.* **8** 3390
18. Thomas J, Kumar D and Ramanan A 2013 Crystallization of phosphomolybdate clusters mediated by copper azole complexes: Influence of pH and temperature *Inorg. Chim. Acta* **396** 126
19. Thomas J and Ramanan A 2011 Phosphomolybdate cluster based solids mediated by transition metal complexes *Inorg. Chim. Acta* **372** 243
20. Moulton B and Zaworotko MJ 2001 From molecules to crystal engineering: supramolecular isomerism and polymorphism in network solids *Chem. Rev.* **101** 1629
21. Nakamoto K 1978 *Infrared and Raman Spectra of Inorganic and Coordination Compounds* (John Wiley & Sons: New York)
22. Bruker Analytical X-ray Systems, SMART: Bruker Molecular Analysis Research Tool, Version 5.618, 2000
23. Bruker Analytical X-ray Systems, SAINT-NT, Version 6.04, 2001
24. Bruker Analytical X-ray Systems, SHELXTL-NT, Version 6.10, 2000
25. Klaus B., University of Bonn, Germany DIAMOND, Version 4.1
26. Strandberg R 1973 The molecular and crystal structure of $Na_6Mo_5P_2O_{23}(H_2O)_{13}$ a compound containing sodium-coordinated pentamolybdodiphosphate anions *Acta Chem. Scand.* **27** 1004
27. Shi Z, Li F, Zhao J, Yu ZY, Zheng Y, Chen Z, *et al.* 2019 A 3D inorganic-organic hybrid constructed from Strandberg-type polyoxometalates and silver complexes: Synthesis, structure and properties *Inorg. Chem. Commun.* **102** 104
28. Shi S, Chen L, Zhao X, Ren B, Cui X and Zhang J 2018 Role of H-bonds in the crystal packing of three novel Strandberg-type polyoxoanion compounds *Inorg. Chim. Acta* **482** 870
29. Xia X, Xia L, Zhang G, Jiang Y, Sun F and Wu H 2021 A 2-D Zn(II) coordination polymer based on 4,5-imidazoledicarboxylate and bis(benzimidazole) ligands: synthesis, crystal structure and fluorescence properties *Z. Naturforsch.* **76B** 313
30. Zhou Y F, Lou B Y, Yuan D Q, Xu Y Q, Jiang F L and Hong M C 2005 pH-value-controlled assembly of photoluminescent zinc coordination polymers *Inorg. Chim. Acta* **358** 3057
31. Kani I 2012 Unusual Very Strong O–H...O Hydrogen Bonding in Zinc Complex: Crystal Structure and Photoluminescence of $[Zn(HL)(bpy)_2(H_2O)]_2(L)$ (L = $O_2C(CF_2)_6CO_2$, bpy = 2,2'bipyridine) *J. Chem. Crystallogr.* **42** 832
32. Liu H Y, Wu H, Ma J F, Liu Y Y, Liu B and Yang J 2010 Syntheses, Structures, and Photoluminescence of Zinc(II) Coordination Polymers Based on Carboxylates and Flexible Bis-[(pyridyl)-benzimidazole] Ligands *Cryst. Growth Des.* **10** 4795
33. Singh N and Anantharaman G 2014 Coordination polymers built with transition metal sulphates and angular 2,5-bis(imidazol-1-yl)thiophene($thim_2$): synthesis, structure and photoluminescent properties *CrystEngComm* **16** 6203
34. Zhang J, Xie Y R, Ye Q, Xiong R G, Xue Z and You X Z 2003 Blue to Red Fluorescent Emission Tuning of a Cadmium Coordination Polymer by Conjugated Ligands *Eur. J. Inorg. Chem.* 2572
35. Dewick P M 2006 *Essentials of organic chemistry: for students of pharmacy medicinal chemistry and biological chemistry* (Wiley: London)
36. Jadon M, Srivastava M, Roy P K and Ramanan A 2021 From molecules to materials: Structural landscape of zinc terephthalates grown from solution *J. Chem. Sci.* **133** 93